SUPPLEMENTARY MATERIAL

Mass spectrometry analysis.

Each lane was systematically cut into 8-10 homogenous slices (fractions) and subjected to in-gel tryptic digestion using modified porcine trypsin (Promega, France) at 20 ng/µl as previously described (1). The dried peptide extracts obtained were dissolved in 14 µl of 0.05% trifluoroacetic acid in 10% acetonitrile and analysed by online nanoLC using an Ultimate 3000 system (Dionex, Amsterdam, The Netherlands) coupled to an nanospray LTQ Orbitrap XL mass spectrometer (Thermo Fisher Scientific, Bremen, Germany). 5µl of each peptide extract were loaded on a 300 µm ID x 5mm PepMap C18 precolumn (LC Packings, Dionex, USA) at 20 µl/min in 2% acetonitrile, 0.05% trifluoroacetic acid. After 5 minutes desalting, peptides were online separated on a 75 µm ID x 15 cm C18 PepMap™ column (LC Packings, Dionex, USA). The flow rate was set at 300 nl/min. Peptides were eluted using a 0 to 50% linear gradient of solvent B in 60 min (solvent A was 0.2% formic acid in 5% acetonitrile and solvent B was 0.2% formic acid in 80% acetonitrile). The LTQ Orbitrap was operated in data-dependent acquisition mode with the XCalibur software (version 2.0 SR2, Thermo Fisher Scientific), using a 60 s dynamic exclusion window to prevent repetitive selection of the same peptide. The survey scan MS was performed in the Orbitrap on the 300-2000 m/z mass range with the resolution set to a value of 60 000 at m/z 400. The five most intense ions per survey scan were selected for MS/MS fragmentation and the resulting fragments were analyzed in the linear trap (parallel mode). The Mascot Daemon software (version 2.2.0, Matrix Science, London, UK) was used for protein identification in batch mode by searching against a non-redundant SwissProt and Trembl Human databases implemented with the SAF-A RDB-GFP-FLAG recombinant protein sequence. Peak lists extraction from Xcalibur raw files were automatically performed through the Mascot Daemon interface using ExtractMSN macro (Thermo Fischer Scientific). Cysteine carbamidomethylation was set as a fixed modification and methionine oxidation, serine/threonine phosphorylation and arginine dimethylation as variable modifications. Up to two missed trypsin cleavages were allowed. Mass tolerances in MS and MS/MS were set to 5 ppm and 0.8 Da, respectively. Mascot results were parsed with the in-house developed software Mascot File Parsing and Quantification (MFPaQ) version 4.0 (2), and protein hits were automatically validated if they satisfied one of the following criteria: identification with at least one top ranking peptide with a Mascot score of more than 49 (p value < 0.001) or at

least two top ranking peptides with a Mascot score of more than 32 (p value < 0.05) and with peptides each of a minimal length of 6 amino acids.

From all the validated result files corresponding to the fractions of a 1D gel lane, MFPaQ was used to generate a unique, non-redundant list of proteins. The software compares proteins or protein groups (composed of all the proteins matching the same set of peptides) and creates clusters from protein groups found in different gel slices if they have one common member. This feature allowed a global list to be edited of unique proteins (or clusters) representing the entire sample analyzed in each gel lane. The global protein lists obtained from the two biological samples from HT1080 cells stably expressing a flag-tagged GFP- SAF-A RDB were compared to extract a list of common proteins. In the same way, this new list was compared to the control protein list from the HT1080 cells stably expressing a flag-tagged GFP to extract the list of specific proteins from HT1080 cells stably expressing a flag-tagged GFP- SAF-A RDB corresponding to the partners of SAF-A RDB domain (supplementary table S4).

SUPPLEMENTARY FIGURE LEGENDS :

Figure S1. SAF-A dynamics in response to DNA damage and identification of partners.

A/ Analyzis by immunofluorescence of XRCC4 dynamics and of PAR production at stripes of laser damage 2 min after microirradiation in HT1080 cells pretreated or not with PARPi (DPQ). Scale bar, 20 μm. **B/** PAR-binding assay on membrane. Extracts from HT1080 cells stably expressing of FLAG-GFP (1), SAF-A-WT-FLAG-GFP (2), SAF-A-dRBD-FLAG-GFP (3), and SAF-A-RBD-FLAG-GFP (4) were electro-transferred on membrane in duplicate. One membrane was botted with anti-GFP antibody and the other incubated with PAR, washed and then blotted with anti-PAR antibody. **C/** Analyzis by immunofluorescence of RNA Pol II and γH2AX, 1 and 10 min after microirradiation in HT1080 cells. Scale bar, 10 μm. **D/** Time-course of fluorescence variation in the non-irradiated nuclear area in laser-irradiated HT1080 cells expressing SAF-A-GFP under PARPi (DPQ) treatment. Images were obtained at 22 s intervals and fluorescence intensities in the non-irradiated and irradiated areas were quantified at each time point. Mean values with SEM of the percentage of fluorescence in the non-irradiated nuclear area vs total nuclear fluorescence were calculated from measurements of 16 independent cells. **E/** HT1080 cells were mock-treated or treated with 10 nM Cali for the indicated time in min or for 1 h followed by incubation in fresh medium for the indicated post-teatment time. Cells were then fractionated as described in the material and methods

section, leading to isolation of the chromatin fractions 4 (F4). Protein samples were denatured and separated on SDS-PAGE gel, followed by electrotransfer and blotting as indicated. **F/** Gel staining after separation of inputs and immunoprecipitates of extracts of HT1080 cells expressing SAF-A-RBD-FLAG-GFP (RBD) or FLAG-GFP (Crtl) as indicated. **G**/ Interaction landscape representing proteins reproducibly co-immunoprecipitated with the RBD domain of SAF-A. To the new interactions identified here were implemented previously known interactions as reported in the String database and in the litterature. The legends « proteins whose depletion increases γH2AX » and « proteins found in PAR co-IP » refer to references (3) and (4), respectively. The proteins excluded from damaged chromatin where reported in the present data and in references (5-7).

Figure S2. Links between transcription and dynamics of SAF-A or FUS in response to DNA damage.

A/ FRAP curves on undamaged or laser-irradiated areas. FRAP experiments were performed on HT1080 cells expressing SAF-A-GFP and pretreated with DPQ. The same nuclear strip was bleached before (non-irradiated area) and 2 min after pulsed laser micro-irradiation (irradiated area, corresponding to SAF-A-GFP exclusion area). The graph shows FRAP curves of mean values with SEM of 44 independent fluorescence measurements. **B/** Monitoring transcription by incorporation of EU in HT1080 cells in the presence of DRB, Actinomycin D or α-amanitin. Scale bar, 20 µm. **C/** Effect of DNA damage by calichemicin (Cali) and/or transcription inhibition (DRB) on FRAP curve for SAFA-GFP. Images were obtained at 487 ms intervals. The data were normalized to the prebleach fluorescence level. The graph shows FRAP curves of mean values with SEM of 29, 29, 24 and 31 independent fluorescence measurements for conditions with DRB, DRB + Cali, Cali and no agent, respectively. **D/** HT1080 cells grown on glass slides were permeabilized in buffer containing or not RNAseA prior to fixation. Then cells were immunostained for nucleolin. Scale bar, 20 µm. **E/** HT1080 cells expressing SAF-A-GFP and grown on glass slides were laser irradiated. After 2 min, cells were permeabilized in buffer containing or not RNAseA prior to fixation. Then cells were immunostained for γH2AX and the DNA stained with propidium iodide. Scale bar, 20 µm. **F/** Effect of a PARPi (DPQ) and a transcription inhibitor (actinomycin D) on the dynamics of SAF-A-GFP at laser-damaged sites. Images were obtained at 22 s intervals, and fluorescence intensities at the damage sites were quantified. Mean values of the fluorescence intensities with SEM were calculated from 16, 20 and 28 independent measurements for conditions with actinomycin D, actinomycin D+DPQ and DPQ,

respectively. **G/** Effect of a transcription inhibitor (DRB) on dynamics of SAF-A-GFP and FUS-GFP at laser-damaged sites in the presence of PARPi (DPQ). Images were obtained at 22 s intervals, and fluorescence intensities at the damage sites were quantified. Mean values of the fluorescence intensities with SEM were calculated for SAF-A-GFP from 25 and 21 independent measurements for conditions with and without DRB, respectively and for FUS-GFP from 25 and 21 independent measurements for conditions with and without DRB, respectively. **H/** Monitoring transcription by incorporation of EU in HT1080 cells under control conditions or in the presence of DPQ or DPQ and PIKKS inhibitors. Scale bar, 20 μm.

Figure S3. A/ Effect of transcription inhibition (actinomycin D) on FRAP curve for mutant mCherry-RNAseHI. Images were obtained at 487 ms intervals. The data were normalized to the prebleach fluorescence level. The graph shows FRAP curves of mean values with standard deviation of 23 and 29 independent fluorescence measurements for conditions without or with actinomycin D, respectively. **B/** Dynamics of mutant RNaseHI at laser-damaged sites in HT1080 cells was measured in the presence or not of diospyrin D1 as indicated. Images were obtained at 7.75 s intervals, and fluorescence intensities at the damage sites were quantified. Mean values of the fluorescence intensities with SEM were calculated from 17 and 20 independent measurements for conditions with and without diospyrin, respectively. **C/** Effect of diospyrin D1 on dynamics of SAF-A-GFP at laser-damaged sites. Images were obtained at 7.75 s intervals, and fluorescence intensities at the damage sites were quantified. Mean values of the fluorescence intensities with SEM were calculated from 52 and 47 independent measurements for conditions with and without diospyrin, respectively. **D/** Effect of diospyrin D1 on dynamics of SAF-A-GFP at laser-damaged sites in the presence of PARPi (DPQ). Images were obtained at 7.75 s intervals, and fluorescence intensities at the damage sites were quantified. Mean values of the fluorescence intensities with SEM were calculated from 32 and 22 independent measurements for conditions with and without diospyrin, respectively.

SUPPLEMENTARY REFERENCES

1. Shevchenko, A., Wilm, M., Vorm, O. and Mann, M. (1996) Mass spectrometric sequencing of proteins silver-stained polyacrylamide gels. *Anal Chem*, **68**, 850-858.
2. Bouyssie, D., Gonzalez de Peredo, A., Mouton, E., Albigot, R., Roussel, L., Ortega, N., Cayrol, C., Burlet-Schiltz, O., Girard, J.P. and Monsarrat, B. (2007) Mascot file parsing and quantification (MFPaQ), a new software to parse, validate, and quantify proteomics data generated by ICAT and SILAC mass spectrometric analyses: application to the proteomics study of membrane proteins from primary human endothelial cells. *Mol Cell Proteomics*, **6**, 1621-1637.

3. Paulsen, R.D., Soni, D.V., Wollman, R., Hahn, A.T., Yee, M.C., Guan, A., Hesley, J.A., Miller, S.C., Cromwell, E.F., Solow-Cordero, D.E. *et al.* (2009) A genome-wide siRNA screen reveals diverse cellular processes and pathways that mediate genome stability. *Mol Cell*, **35**, 228-239.
4. Gagne, J.P., Isabelle, M., Lo, K.S., Bourassa, S., Hendzel, M.J., Dawson, V.L., Dawson, T.M. and Poirier, G.G. (2008) Proteome-wide identification of poly(ADP-ribose) binding proteins and poly(ADP-ribose)-associated protein complexes. *Nucleic Acids Res*, **36**, 6959-6976.
5. Adamson, B., Smogorzewska, A., Sigoillot, F.D., King, R.W. and Elledge, S.J. (2012) A genome-wide homologous recombination screen identifies the RNA-binding protein RBMX as a component of the DNA-damage response. *Nat Cell Biol*, **14**, 318-328.
6. Beli, P., Lukashchuk, N., Wagner, S.A., Weinert, B.T., Olsen, J.V., Baskcomb, L., Mann, M., Jackson, S.P. and Choudhary, C. (2012) Proteomic Investigations Reveal a Role for RNA Processing Factor THRAP3 in the DNA Damage Response. *Mol Cell*, **46**, 212-225.
7. Polo, S.E., Blackford, A.N., Chapman, J.R., Baskcomb, L., Gravel, S., Rusch, A., Thomas, A., Blundred, R., Smith, P., Kzhyshkowska, J. *et al.* (2012) Regulation of DNA-End Resection by hnRNPU-like Proteins Promotes DNA Double-Strand Break Signaling and Repair. *Mol Cell*, **45**, 505-516.

SUPPLEMENTARY TABLES :

Table S1 : list of primers used.

ID	Sequence	Restriction site(s)
FLAG-S	GATCCGCCGCCACCATGACGCGTGATTACAAGGATGACGACGATAAGCCA	BamHI MluI
FLAG-AS	CCGGTGGCTTATCGTCGTCATCCTTGTAATCACGCGTCATGGTGGCGGCG	BamHI MluI
SAFA-F	CCGGATCCGCCGCCACCATGAGTTCCTCGCCTG	BamHI
SAFA-R	CCGACGCGTATGCATATAATATCCTTGGTGATAATGC	MluI
SAFAdDBD-F	CCGGATCCGCCGCCACCATGGATAAAAAGAGGGGTGTTAAAAGACC	BamHI
SAFAdRBD-R	CCACGCGTAAGAGCCTTTTTGCTTTCTTCC	MluI
SAFA-RBD-F	CCGGATCCGCCGCCACCATGCCACCAGAAAAGAAACAGAACACTGGC	BamHI
FUS-F	CCGGATCCGCCGCCACCATGGCCTCAAACGATTATACCCAACAAGC	BamHI
FUS-R	GCCACGCGTATACGGCCTCTCCCTGCGATCCTGTCTGTGCTCACC	MluI
NLS-S	AGCTTGCCACCATGACGCGTGGCCCCAAGAAAAAGCGGAAAGTGGGA	HindIII AgeI
NLS-AS	CCGGTCCCACTTTCCGCTTTTTCTTGGGGCCACGCGTCATGGTGGCA	HindIII AgeI

Table S2 : list of antibodies used.

Antibody	Host	Source	Clone/catalog	Use
β-actin	Mouse	Ambion	AC-15	WB: 1/10 000
DNA ligase IV	Rabbit	AbD Serotec	AHP554	WB: 1/2000
Ph-DNA-PKcs (S2056)	Rabbit	Abcam	ab18192	WB: 1/200
FLAG	Mouse	Sigma-Aldrich	M2 / F-1804	WB: 1/1000
FUS/TLS	Mouse	BD Biosciences	15/TLS / 611385	IF: 1/40 WB: 1/1000
GFP-booster	Synthetic	Chromotek	gba488	IF: 1/200
γH2AX (S139)	Mouse	Millipore	JBW301 / 05-636	IF: 1/500

				WB: 1/1000
γH2AX (S139)	Rabbit	Assay designs	905 771 100	IF: 1/1000
HP-1α	Mouse	gift from R. Losson, IGBMC, Illkirch, France	2HP-2G9	WB: 1/2000
Ku80	Mouse	Abcam	S10B1 / ab2173	WB: 1/1000
mCherry	rabbit	Abcam	ab62341	IF: 1/800 WB: 1/1000
Nucleolin/C23	rabbit	Santa Cruz Biotech.	H-250 / sc-13057	IF: 1/300
PAR	Rabbit	BD Pharmingen	551813	WB: 1/2000
PAR	Mouse	Trevigen	4335-AMC	IF : 1/200
RNA pol. II	Mouse	Santa Cruz Biotech.	8WG16 / sc-56767	IF: 1/25 WB: 1/100
SAF-A	Mouse	Santa Cruz Biotech.	3G6 / sc-32315	IF: 1/300 or 1/100 with pre-extraction WB: 1/100
TAF15/TAFII68	Mouse	Eurogentec	7TA-2B11 / IGTAF-2B11	IF : 1/100 or 1/200 with pre-extraction WB: 1/1000
XRCC4	Rabbit	Home-made serum	NA	WB: 1/1000
RNA :DNA hybrids	Mouse	gift from Dr SH Leppla NIH, Bethesda, MD, USA	S9.6	IF : 1/100

NA: not applicable.

Table S3: list of inhibitors used.

Inhibitor	Global target	Source	Stock	Use
DPQ	PAR synthesis	Sigma-Aldrich	16.5 mM/DMSO	40 µM 2h
NU1025	PAR synthesis	Calbiochem	100 mM/DMSO	100 µM 30 min
DRB	Transcription	Sigma-Aldrich	31 mM/DMSO	100 µM 2 h
actinomycin D	Transcription	Sigma-Aldrich	5 mM/DMSO	2.25 µg/ml 40 min
α-amanitin	Transcription	Sigma-Aldrich	1 mg/ml /H2O	50 µg/ml 5 h
NU7441	DNA-PK	Tocris-Bioscience	5 mM /DMSO	10 µM 1 h
KU55933	ATM	Tocris-Bioscience	10 mM/DMSO	15 µM 1 h
VE-821	ATR	Tinib-tools	10 mM/DMSO	20 µM 25 min
Diospyrin D1	Spliceosome assembly	Gift from B. Hazra, Jadavpur University, Calcutta, India	5 mM/DMSO	10 µM 24 h

Table S4 : proteins associated to the C-terminal RBD SAF-A domain.

Protein name	Gene name	Best score[a]	Number of peptides[b]	Sequence Coverage (%)
Spectrin alpha chain, brain	SPTAN1	1800	97	44
Splicing factor 3B subunit 2	SF3B2	1880	86	59
Neuroblast differentiation-associated protein AHNAK	AHNAK	708	72	14
Splicing factor 3B subunit 3	SF3B3	1750	66	54
Splicing factor, proline- and glutamine-rich	SFPQ	879	56	54
Splicing factor 3A subunit 1	SF3A1	926	51	57
Superkiller viralicidic activity 2-like 2	SKIV2L2	710	51	47
Putative uncharacterized protein DKFZp762M013 (Fragment)	DKFZp762M013	442	50	58
Heterogeneous nuclear ribonucleoprotein U-like protein 1	HNRNPUL1	1247	49	47
AP-2 complex subunit beta	AP2B1	773	41	49
Polyadenylate-binding protein 1	PABPC1	699	40	61
Heterogeneous nuclear ribonucleoprotein U	HNRNPU	463	39	35
cDNA FLJ54492, highly similar to Eukaryotic translation initiation factor 4B		443	38	52
Interleukin enhancer-binding factor 3	ILF3	470	36	43
Heterogeneous nuclear ribonucleoprotein A1	HNRNPA1	807	34	61
TAF15 RNA polymerase II, TATA box binding protein (TBP)-associated factor, 68kDa, isoform CRA_a	**TAF15**	**387**	**34**	**55**
Thyroid hormone receptor associated protein 3, isoform CRA_a	THRAP3	227	33	31
Cleavage stimulation factor subunit 3	CSTF3	696	29	43
Plasminogen activator inhibitor 1 RNA-binding protein	SERBP1	621	29	60
WD40 repeat-containing protein SMU1	SMU1	279	29	48
Pre-mRNA-processing factor 19	PRPF19	689	27	65
Far upstream element-binding protein 1	FUBP1	330	27	43
Heterogeneous nuclear ribonucleoprotein A3	HNRNPA3	710	25	39
cDNA FLJ55635, highly similar to pre-mRNA-splicing factorATP-dependent RNA helicase DHX15 (EC 3.6.1.-)		405	25	28
Heterogeneous nuclear ribonucleoproteins A2/B1	HNRNPA2B1	681	24	69
cDNA FLJ46581 fis, clone THYMU3043200, highly similar to Splicing factor 3A subunit 3		402	24	48
Heterogeneous nuclear ribonucleoprotein Q	SYNCRIP	367	24	45
cDNA, FLJ92657, highly similar to Homo sapiens heterogeneous nuclear ribonucleoprotein C (C1/C2) (HNRPC), transcript variant 2, mRNA		261	21	55
Bcl-2-associated transcription factor 1	BCLAF1	118	20	18
RNA-binding protein FUS	**FUS**	**313**	**18**	33
Heterogeneous nuclear ribonucleoprotein H	HNRNPH1	238	18	49
cDNA FLJ30038 fis, clone 3NB692001511, highly similar to Homo sapiens heterogeneous nuclear	HNRPAB	279	18	42

ribonucleoprotein A/B (HNRPAB), transcript variant 2, mRNA				
Pre-mRNA-processing factor 17	CDC40	209	18	38
Splicing factor 3A subunit 2	SF3A2	189	17	27
Transcription elongation regulator 1	TCERG1	81	16	13
Replication protein A 70 kDa DNA-binding subunit	RPA1	234	14	34
Splicing factor 3B subunit 4	SF3B4	479	12	32
Cyclin-K	CCNK	214	12	24
Salt-tolerant protein	STP	134	11	25
Myosin regulatory light chain 12A	MYL12A	209	10	55
Splicing factor 3B subunit 5	SF3B5	133	8	91
Neurabin-2	PPP1R9B	132	8	10
Pre-mRNA branch site protein p14	SF3B14	110	6	41
Transitional endoplasmic reticulum ATPase	VCP	96	6	10
HCG2039797 (Fragment)	Tcr-alpha	321	2	38

[a] The best Mascot protein score is given when the protein was identified in several 1D gel fractions from one of the replicate sample

[b] The total number of unique peptides assigned to a protein in the 1D gel fraction where it showed the best Mascot score and sequence coverage.

Proteins displayed in bold correspond to the coprecipitated proteins, FUS/TLS and TAFII68/TAF15, chosen for further analysis.

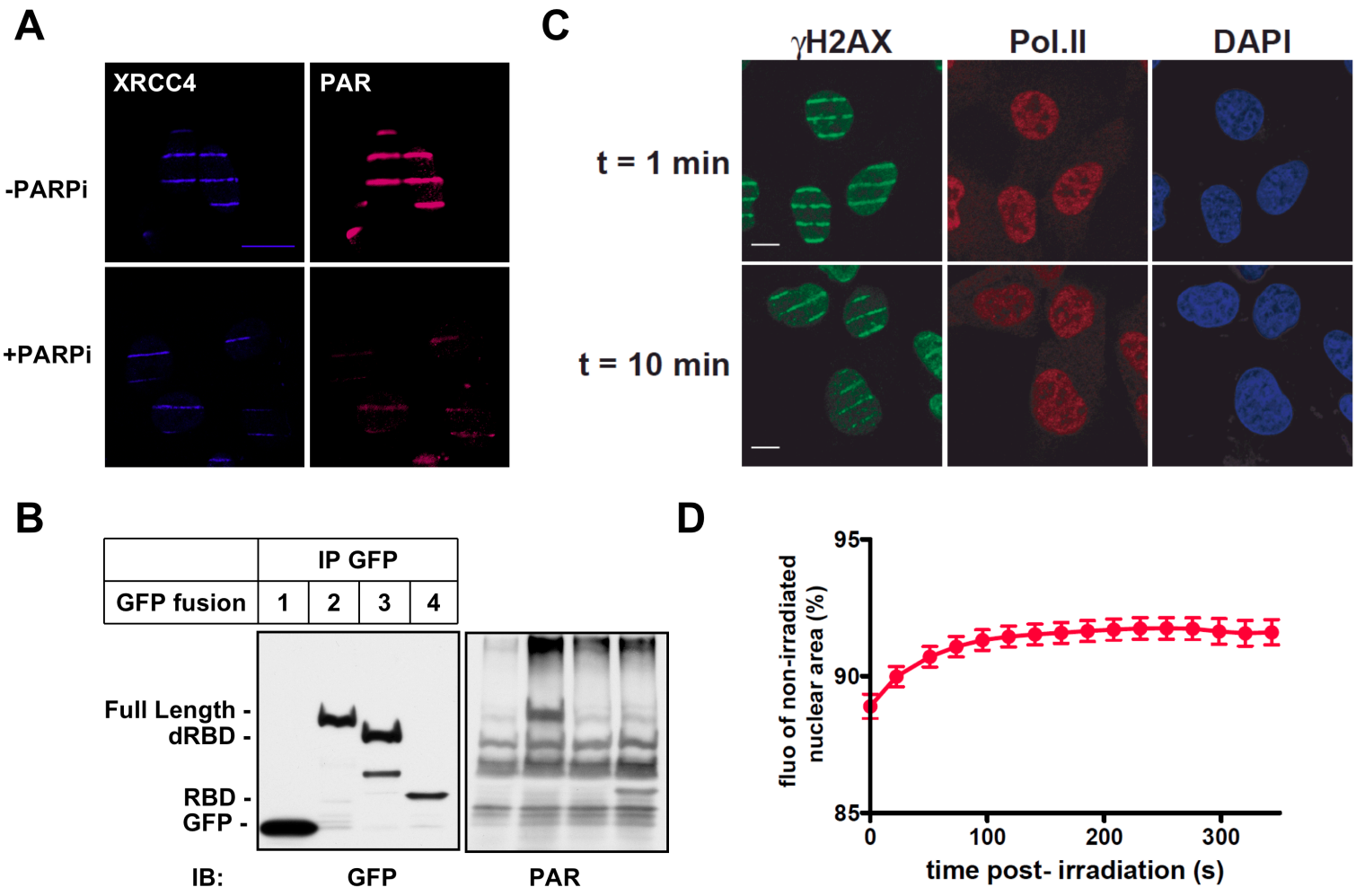

Supplementary Figure S1

E

Fraction	F4										
Post-Treatment (h)	-	-	-	-	-		1	2	3	4	-
Treatment Time (min)	-	5	15	30	60		60	60	60	60	-

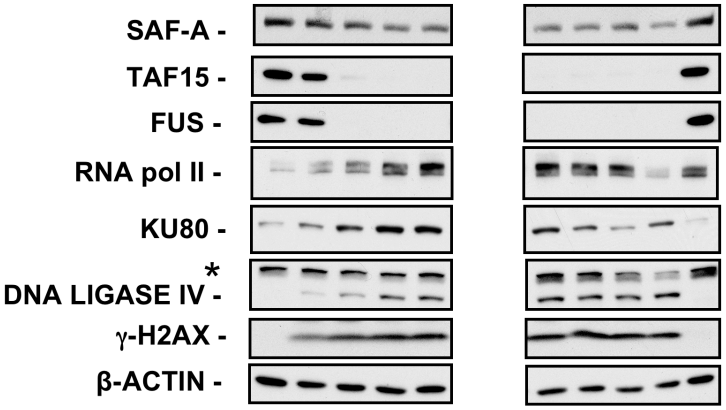

F

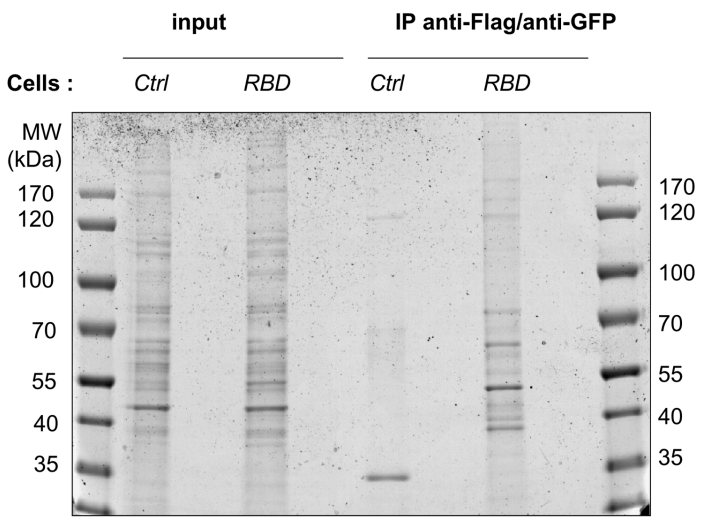

Supplementary Figure S1

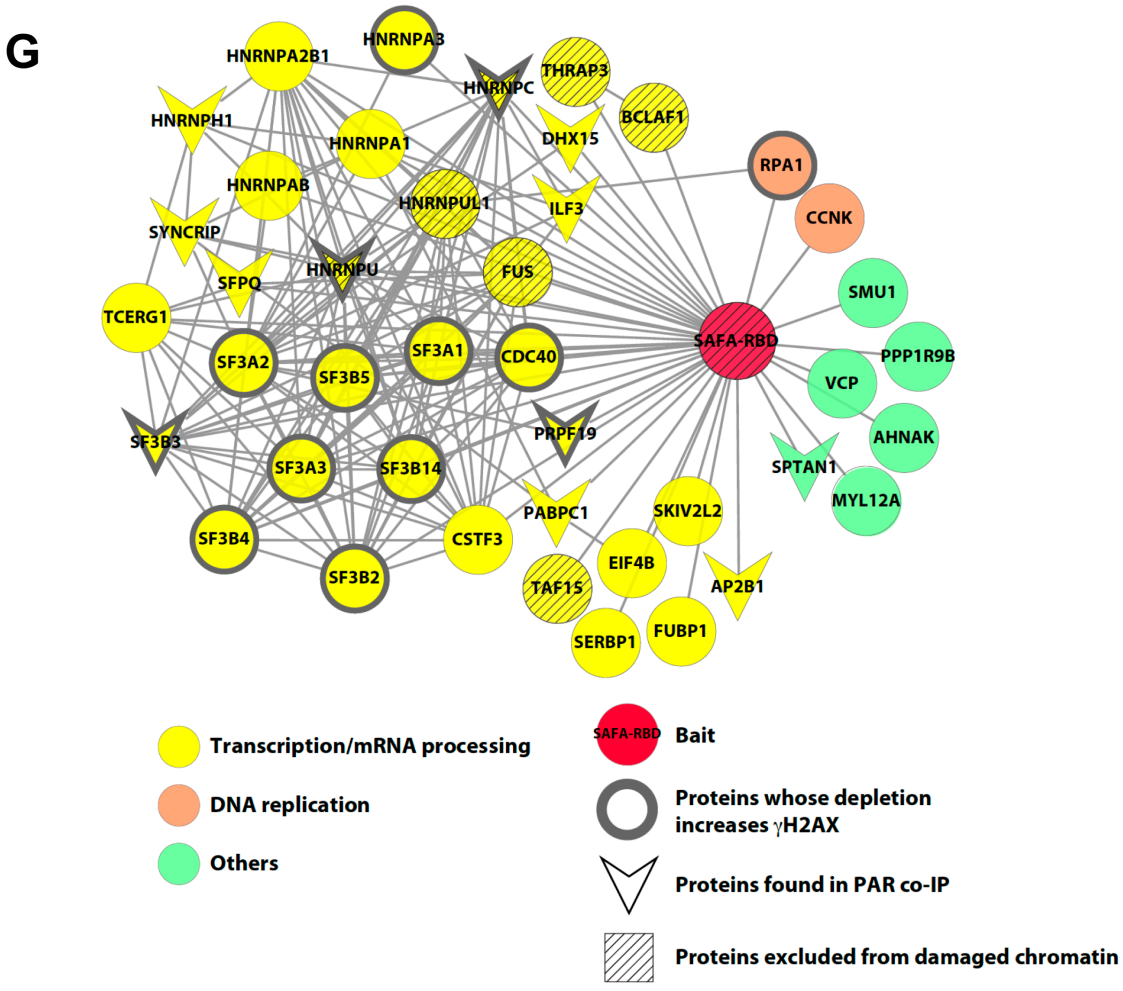

Supplementary Figure S1

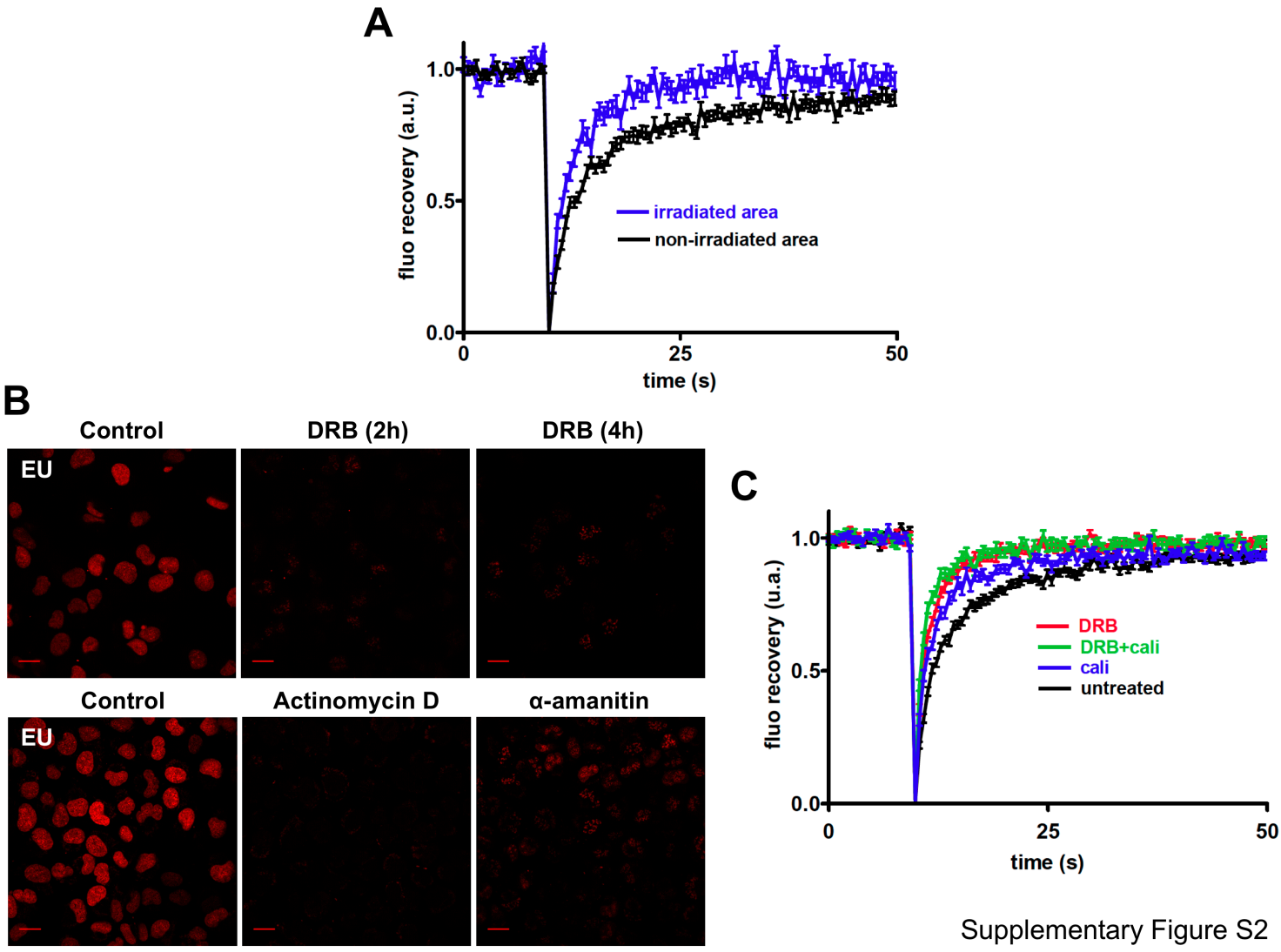

Supplementary Figure S2

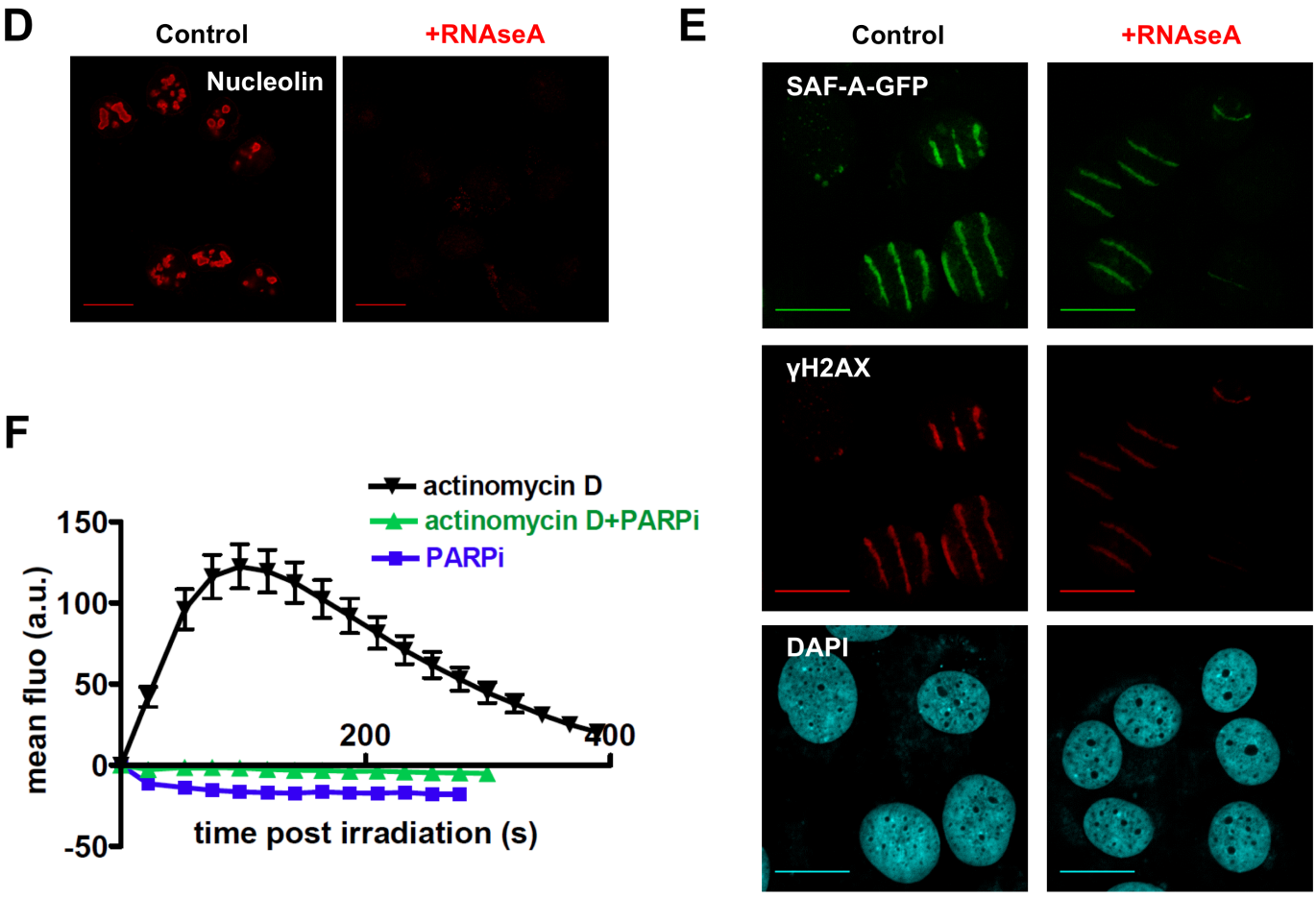

Supplementary Figure S2

G

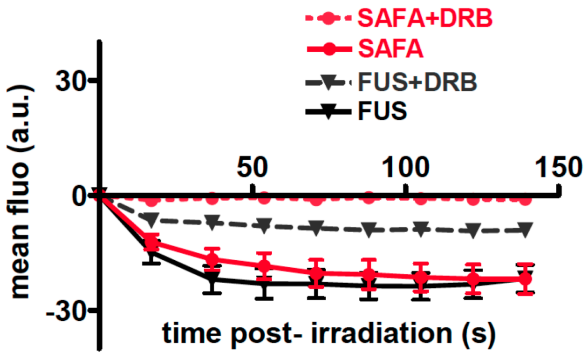

H

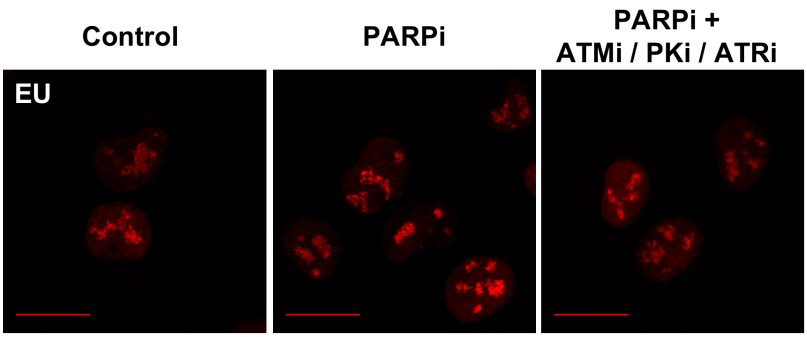

Supplementary Figure S2

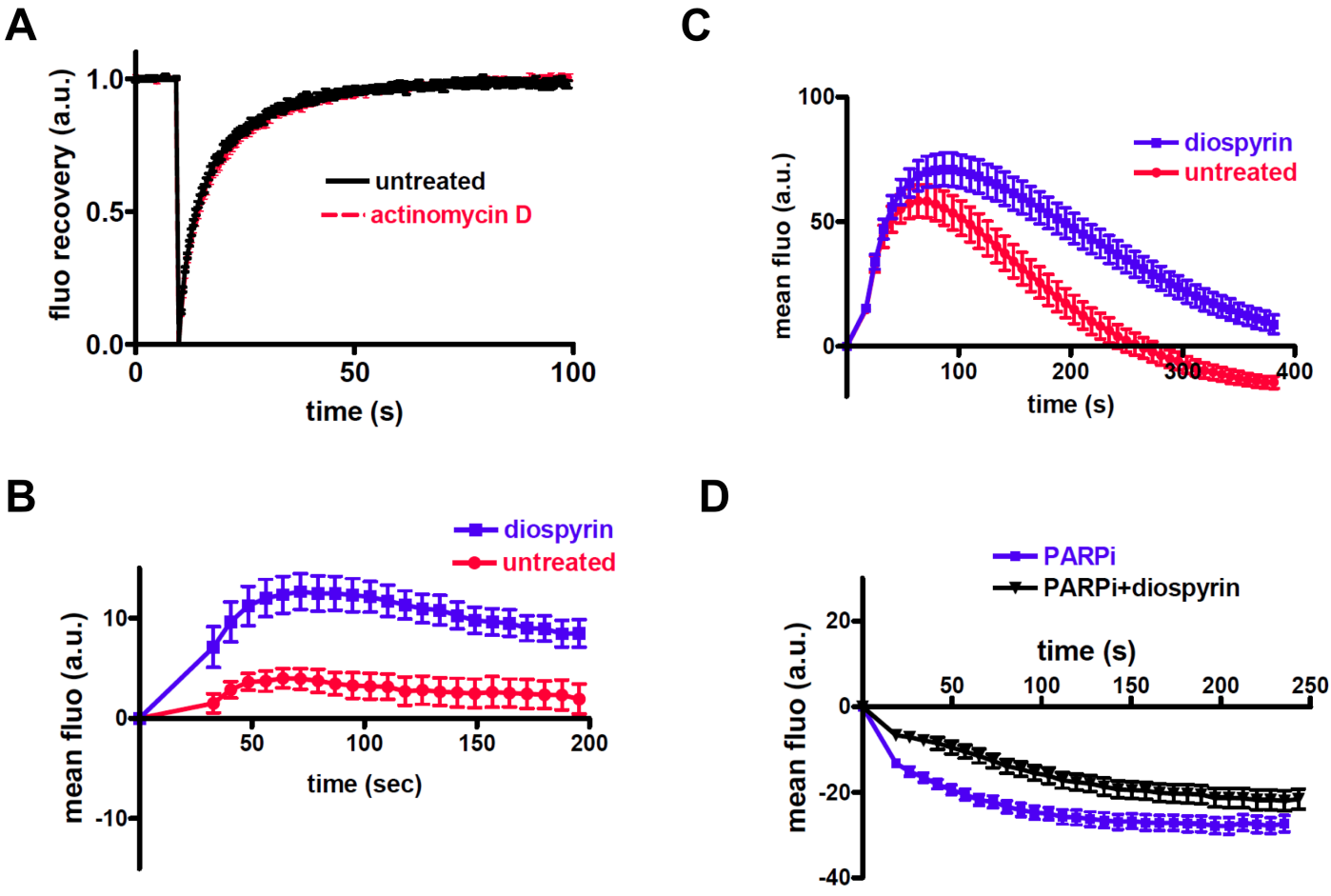

Supplementary Figure S3